6-5-2014

Spring hydrology determines summer net carbon uptake in northern ecosystems

Yonghong Yi
University of Montana - Missoula

John S. Kimball
University of Montana - Missoula

Rolf H. Reichle
NASA

Recommended Citation

Yi, Yonghong; Kimball, John S.; and Reichle, Rolf H., "Spring hydrology determines summer net carbon uptake in northern ecosystems" (2014). *Biological Sciences Faculty Publications*. 407.
https://scholarworks.umt.edu/biosci_pubs/407

OPEN ACCESS
IOP Publishing
Environmental Research Letters
Environ. Res. Lett. **9** (2014) 064003 (11pp)
doi:10.1088/1748-9326/9/6/064003

Spring hydrology determines summer net carbon uptake in northern ecosystems

Yonghong Yi[1,2], **John S Kimball**[1,2] **and Rolf H Reichle**[3]

[1] Flathead Lake Biological Station, The University of Montana, 32125 Biostation Lane, Polson, MT 59860-9659, USA
[2] Numerical Terradynamic Simulation Group, The University of Montana, Missoula, MT 59812, USA
[3] Global Modeling and Assimilation Office, NASA Goddard Space Flight Center, Greenbelt, MD 20771, USA

E-mail: yonghong.yi@ntsg.umt.edu

Received 3 February 2014, revised 10 April 2014
Accepted for publication 9 May 2014
Published 5 June 2014

Abstract

Increased photosynthetic activity and enhanced seasonal CO_2 exchange of northern ecosystems have been observed from a variety of sources including satellite vegetation indices (such as the normalized difference vegetation index; NDVI) and atmospheric CO_2 measurements. Most of these changes have been attributed to strong warming trends in the northern high latitudes ($\geqslant$50° N). Here we analyze the interannual variation of summer net carbon uptake derived from atmospheric CO_2 measurements and satellite NDVI in relation to surface meteorology from regional observational records. We find that increases in spring precipitation and snow pack promote summer net carbon uptake of northern ecosystems independent of air temperature effects. However, satellite NDVI measurements still show an overall benefit of summer photosynthetic activity from regional warming and limited impact of spring precipitation. This discrepancy is attributed to a similar response of photosynthesis and respiration to warming and thus reduced sensitivity of net ecosystem carbon uptake to temperature. Further analysis of boreal tower eddy covariance CO_2 flux measurements indicates that summer net carbon uptake is positively correlated with early growing-season surface soil moisture, which is also strongly affected by spring precipitation and snow pack based on analysis of satellite soil moisture retrievals. This is attributed to strong regulation of spring hydrology on soil respiration in relatively wet boreal and arctic ecosystems. These results document the important role of spring hydrology in determining summer net carbon uptake and contrast with prevailing assumptions of dominant cold temperature limitations to high-latitude ecosystems. Our results indicate potentially stronger coupling of boreal/arctic water and carbon cycles with continued regional warming trends.

S Online supplementary data available from stacks.iop.org/ERL/9/064003/mmedia

Keywords: boreal/arctic, net carbon uptake, spring hydrology, vegetation productivity, respiration, soil moisture

1. Introduction

Northern boreal and arctic ecosystems are an important component of the global carbon cycle, and their sensitivity to climate change remains largely uncertain (McGuire *et al* 2012). Besides a strong warming trend in the northern high latitudes ($\geqslant$50°N), an increase in spring precipitation is also likely to occur (Solomon *et al* 2007), which may have a profound impact on regional ecosystems and the carbon cycle, including photosynthesis, soil litter decomposition and respiration, and disturbance (e.g. fire, insects). Previous studies have largely focused on how warming affects vegetation growth and associated carbon (CO_2) uptake (Angert *et al* 2005, Piao *et al* 2008, Zhang *et al* 2008, Xu *et al* 2013), while few studies of northern ecosystems have addressed how variations in seasonal precipitation and temperature together affect surface hydrology and its impact on net ecosystem carbon uptake. Vegetation greening and increasing carbon uptake associated with warming in the spring have been observed at both field and broad ecosystem scales indicated by tower eddy covariance CO_2 flux measurements, satellite vegetation greenness indices, and atmospheric CO_2 observations (Welp *et al* 2007, Beck and Goetz 2011, Graven *et al* 2013, Xu *et al* 2013). However, how northern vegetation responds to summer temperature increases is uncertain, with both vegetation greening and browning being reported from satellite vegetation indices and similar conflicting findings reported from tower eddy covariance measurements (Angert *et al* 2005, Welp *et al* 2007, Zhang *et al* 2008, Buermann *et al* 2013). A few field studies have shown that surface and subsurface hydrology have a dominant role in regulating the interannual variation of net carbon uptake in both boreal and arctic ecosystems (Desai *et al* 2010, Olivas *et al* 2010, Lupascu *et al* 2013, Sharp *et al* 2013); however, these relatively sparse and short-duration measurements may not be representative of how net ecosystem carbon uptake responds to changes in surface hydrology at regional scales.

The objective of this study is to investigate how spring hydrology and summer temperature affect the interannual variability of summer vegetation growth and regional net carbon (CO_2) uptake in the northern high latitudes (⩾50°N). To that end, we conducted a synthesized analysis of atmospheric CO_2 observations, net ecosystem exchange (NEE) CO_2 fluxes simulated by a global atmospheric Bayesian model inversion system, satellite NDVI measurements, and gridded surface meteorology datasets over the past three decades (from 1979), and more recent tower eddy covariance measured carbon fluxes and satellite surface soil moisture retrievals (2003–2011).

2. Methods and datasets

The seasonal cycle of atmospheric CO_2 in the northern high latitudes is primarily driven by the net ecosystem productivity of underlying terrestrial ecosystems (Randerson *et al* 1997). The atmospheric CO_2 seasonal cycle (⩾50°N) was derived from marine boundary layer (MBL) Reference data available from the National Oceanic and Atmospheric Administration (NOAA) Earth System Research Laboratory (ESRL). This dataset is based on measurements from a subset of sites from the NOAA Cooperative Global Air Sampling Network representing well-mixed MBL air samples of a large volume of atmosphere (Masarie *et al* 1995). First a smooth curve was fitted to the weekly atmospheric flask CO_2 measurements to reduce the effects of synoptic-scale atmospheric variability, and the records were extended to synchronize the time series and fill temporal data gaps. Latitudinal distributions of CO_2 concentrations and zonal-averaged reference conditions were then constructed based on the smoothed and extended MBL flask records (Masarie *et al* 1995). The detrended atmospheric CO_2 seasonal cycle was extracted from these weekly CO_2 concentration records following Thoning *et al* (1989). Generally, for the northern high latitudes, the spring zero-crossing timing of the mean CO_2 seasonal cycle occurs at the end of June, and the CO_2 concentration reaches a minimum at the end of August due to the seasonal drawdown of atmospheric CO_2 by vegetation net photosynthesis. This summer CO_2 minimum (CO_2_sum_min) was used as a surrogate for ecosystem net photosynthetic carbon uptake occurring from June to August (Angert *et al* 2005).

We also examined the CO_2 seasonal cycle of northern ecosystems simulated by a long-term global atmospheric inversion system (Chevallier *et al* 2010; available from 1979 to 2011). In this system, surface CO_2 mixing ratio measurements from more than 128 stations were assimilated using a Bayesian framework and a Monte Carlo approach to infer the fluxes and their error statistics on a 3.75° × 2.5° (longitude-latitude) grid. The analyzed zonal-averaged (⩾50°N) monthly NEE fluxes were used to examine relations between climate controls and northern summer (JJA, from June to August) net carbon uptake for the past three decades.

Satellite vegetation greenness indices like the NDVI have been widely used as a surrogate for vegetation gross primary productivity (e.g. Beck and Goetz 2011, Buermann *et al* 2013, Xu *et al* 2013). A long-term global 8 km bimonthly satellite NDVI dataset (1982–2010) was obtained from the third-generation Global Inventory Monitoring and Modelling Studies (GIMMS3g) dataset (Xu *et al* 2013). This dataset was assembled from different NOAA advanced very high resolution radiometer (AVHRR) sensor records, accounting for various deleterious effects including calibration loss, orbital drift and volcanic eruptions. For this analysis, the GIMMS3g data were aggregated to 0.5° spatial resolution and a monthly time step.

Fire emissions are a large component of the boreal carbon cycle (Bond-Lamberty *et al* 2007). Monthly CO_2 fire emissions from 1997 to 2011 were obtained from the Global annual Fire Emission Database version 3 (GFED v.3.1); the GFED fire emissions were generated using a revised Carnegie-Ames-Stanford-Approach (CASA) biogeochemical model and improved satellite-derived estimates of burned areas, fire activity and plant productivity at 0.5° spatial resolution and monthly time step (van der Werf *et al* 2010). The GFED dataset indicates that on average around 70% of fire CO_2 emissions in areas north of 50°N occurs during the period from June to August.

Climate records used in this study include surface air temperature (T) from the 0.5° CRU (Climate Research Unit) TS3.20 dataset (Harris *et al* 2013), precipitation (P) from GPCP (Global Precipitation Climatology Project, version 2.2) 2.5° gridded data (Adler *et al* 2012), and snow water equivalent (SWE) from the Canadian Meteorological Center (CMC) snow depth analysis (Brown and Brasnett 2010). The

CRU dataset is based on climate observations from more than 4000 weather stations around the globe, with relatively few station records in the high latitudes. The GPCP dataset is a merged product combining observations from rain gauge stations with geostationary and polar-orbiting satellite observations at infrared and microwave frequencies. The CMC snow depth analysis merges *in situ* observations, meteorological aviation reports, and special aviation reports with snow model estimates. SWE is estimated from the snow depth analysis using a snow density look-up table. The CMC data are available from August 1998 to December 2012 at a 24 km resolution polar stereographic grid. Both the GPCP precipitation and CMC SWE data were interpolated to 0.5° spatial resolution prior to the analysis.

We tested the dependence of the carbon indices, including NDVI, CO_2_sum_min, fire emissions and model inversion NEE fluxes, on the seasonal climate variables including T, P, and SWE using partial correlation analysis, which was used to account for the co-variation of these climate variables. We chose partial correlation analysis over a multivariate analysis because the meteorology datasets including T, P and SWE are available for different periods. We assume that climate fluctuations are mainly driving annual variations in the summer net carbon uptake of boreal/arctic ecosystems; therefore, all time series were detrended to focus on the co-variation of interannual anomalies of the climate and vegetation parameters for northern vegetated areas defined by the MODIS 500 m global land cover map (MCD12Q1; Friedl *et al* 2010). The non-parametric Mann–Kendall trend detection method was used to detect the trend in each time series, and a trend-free prewhitening analysis was used to account for time series autocorrelation (Yue *et al* 2002). Significant ($p < 0.1$) trends were removed prior to the partial correlation analysis.

Measurements from approximately 23 northern (⩾50°N) eddy covariance (EC) flux towers (table S1) with two or more years of observations covering at least part of the growing season (May–August) were obtained from the global FLUXNET dataset (Baldocchi 2008, Flanagan and Syed 2011); these data were used to analyze local-scale relations between summer net carbon uptake and climate variability. The tower daily carbon flux estimates are derived from half-hourly EC CO_2 flux measurements that are processed and aggregated using consistent gap filling and quality control procedures. Temporal anomalies of summer net carbon uptake at each site are simply the difference of monthly aggregated NEE fluxes from June to August relative to the multi-year (⩾2 years) means.

Daily satellite surface soil moisture retrievals were obtained from an AMSR-E (Advanced Microwave Scanning Radiometer for EOS) global land parameter database developed for ecosystem studies (Jones and Kimball 2010); these data were used to analyze how seasonal climate variations affect surface soil moisture. The soil moisture retrievals were generated at 6.9 GHz and 10.7 GHz wavelengths using an iterative radiative transfer algorithm and multi-frequency AMSR-E brightness temperature inputs under non-precipitating and snow/ice-free conditions (Jones *et al* 2007). The radiative transfer algorithm accounts for surface emissivity variations caused by vegetation roughness and inland and coastal water bodies, which may have a large influence on soil moisture retrievals in the northern high latitudes (Yi *et al* 2011). The AMSR-E soil moisture retrievals are available at 25 km resolution and daily time step from 2003 to 2011. Monthly averaged soil moisture was calculated when there were more than 5 daily retrievals within a given month.

3. Results

3.1. Summer net CO_2 uptake and associated climate controls

The interannual variations of detrended summer (JJA) net CO_2 uptake derived from the MBL atmospheric CO_2 data and spring (MAM, from March to May) precipitation for the zone north of 50°N are shown in figure 1(a). These results indicate that interannual variations in spring precipitation influence summer net carbon uptake, with large spring precipitation anomalies generally associated with strong summer net carbon uptake in the northern high latitudes. Significant negative correlation ($R = -0.55$, $p < 0.001$) was found between the detrended time series of spring precipitation and summer net carbon uptake (figure 1(b)). A weak negative correlation ($R = -0.35$, $n = 13$, $p > 0.1$) was also found between summer net carbon uptake and spring SWE (figure 1(b)). Summer air temperature (T) appears to have only a minimal impact on summer net carbon uptake. Further analysis (table S2) indicates that summer net carbon uptake is most strongly correlated with winter and spring precipitation (from January to May, $R = -0.57$, $p < 0.001$) and peak winter SWE (February, $R = -0.51$, $n = 13$, $p < 0.1$). The results based on atmospheric CO_2 measurements at the 9 northern (⩾50°N) MBL flask sites (table S3) were generally similar to the results based on the MBL reference dataset, i.e. negatively correlated with spring hydrology (P: $R = -0.43 \pm 0.21$; SWE: $R = -0.27 \pm 0.37$), and positively correlated with summer T ($R = 0.17 \pm 0.33$).

The summer NEE fluxes derived from the global atmospheric Bayesian inversion system (Chevallier *et al* 2010) showed a strong positive correlation with summer air temperature ($R = 0.43$, $p < 0.05$), and a weak negative correlation with spring precipitation ($R = -0.21$, $p > 0.1$), and SWE ($R = -0.43$, $n = 13$, $p > 0.1$), as shown by the red bars in figure 1(b). Further analysis (table S2) indicates that the model inversion summer NEE fluxes are most positively correlated with mid-summer air temperature (from July to August, $R = 0.52$, $p < 0.05$), and most negatively correlated with precipitation during winter and early spring (from February to April, $R = -0.33$, $p < 0.1$), and SWE during later spring (from April to May, $R = -0.51$, $n = 13$, $p < 0.1$).

The difference between the results based on the atmospheric CO_2 seasonal cycle and model inversions may be partly due to the variation of atmospheric transport from year-to-year and its impact on the atmospheric CO_2 seasonal cycle, though this impact is relatively small (generally less than 10–15%; Piao *et al* 2008, Graven *et al* 2013) compared to characteristic large variations in the northern CO_2 seasonal

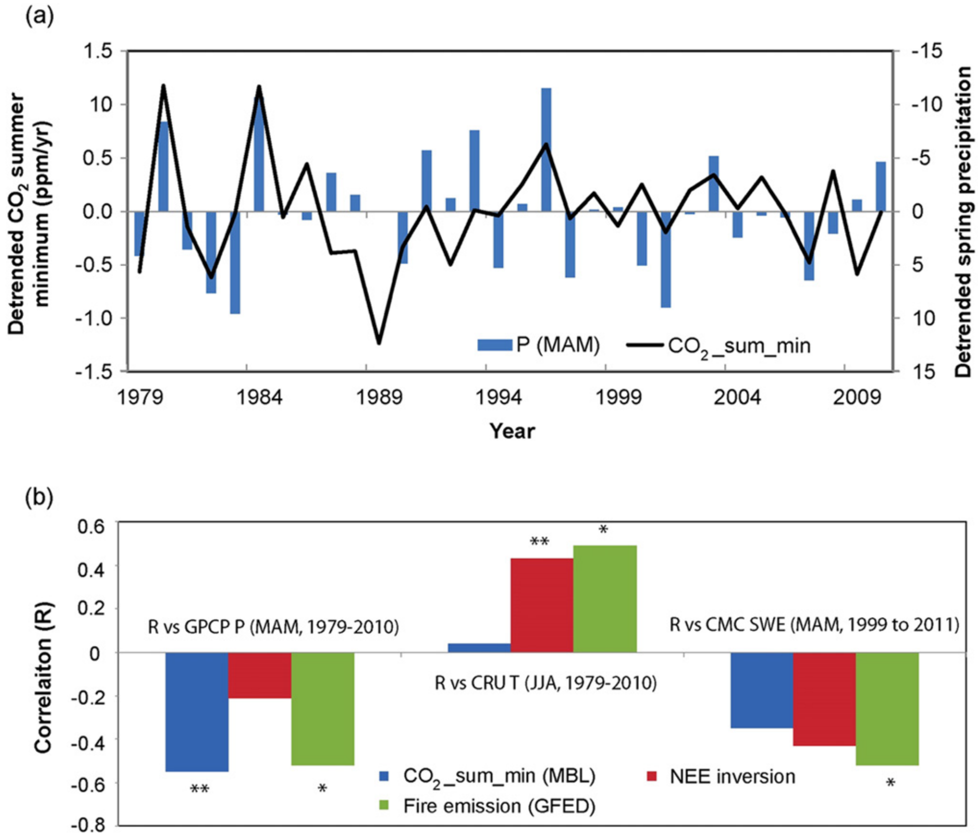

Figure 1. Co-variation of summer net carbon uptake and seasonal climate variables. (a) Time series of detrended summer CO_2 minimum (CO_2_sum_min) derived from NOAA MBL reference data and GPCP spring (MAM) precipitation (P) averaged for zone 50°N to 90°N, where positive (negative) anomalies denote relative decreases (increases) in terrestrial carbon uptake. (b) Partial correlation (R) analysis of carbon fluxes including CO_2_sum_min derived from MBL reference datasets, global atmospheric inversion model estimated NEE fluxes (Chevallier *et al* 2010), and GFED (v.3.1) estimated CO_2 fire emissions versus seasonal climate variables. For the partial correlation analysis against P and SWE, T was used as the controlling variable, while P was used as the controlling variable for the partial analysis against T. All time series were detrended prior to the temporal correlation analysis; asterisks ** and * denote statistical significance at 95% ($p < 0.05$) and 90% ($p < 0.1$) levels, respectively.

cycle. On the other hand, current atmospheric inversion models still have difficulty in clearly distinguishing regional carbon budgets within a continent (Chevallier *et al* 2010, Gurney *et al* 2008), and may not be able to accurately distinguish carbon uptake patterns between the northern middle and high latitudes.

In the high latitudes, fire emissions also contribute to variations in the atmospheric CO_2 seasonal cycle and generally peak in the summer. Large fire emissions generally correspond with reduced summer net carbon uptake indicated by both model inversions and atmospheric CO_2 data (online supplementary figure S1 available at stacks.iop.org/ERL/9/064003). The partial correlation analysis indicates that summer air temperature ($R = 0.49$, $n = 14$, $p < 0.1$) and spring hydrology (for MAM P, $R = -0.52$, $n = 14$, $p < 0.1$; for MAM SWE, $R = -0.52$, $n = 13$, $p < 0.1$) are the two major climatic factors controlling interannual variability of fire emissions in the northern latitudes (table S4).

3.2. Summer NDVI and associated climate controls

The spatial distribution of partial correlation coefficients between detrended satellite-derived summer NDVI and summer T or spring P in the northern latitudes (⩾50°N) is shown in figure 2. Summer NDVI is strongly positively correlated with summer T (figure 2(a)), with relatively weaker correlation with spring T, and overall negligible correlation with both spring and summer P (table S4). The summer NDVI correlation is particularly strong in relation to early summer (June) temperature (figure S2). Moreover, correlations are generally higher for tundra than boreal forest areas (figure 2(c)). Around 60.5%, 23.7% and 21.0% of tundra areas show significant ($p < 0.1$) positive NDVI correlations with respective June, July and August air temperatures, while only 29.4%, 13.1% and 14.4% of boreal forest areas show significant positive correlations for these months (figure S2). On the other hand, summer NDVI is only weakly correlated with spring P (figure 2(b)), with 12.5% of boreal forest areas and 2.9% of tundra areas showing significant positive correlations (figure 2(d)). Similarly, a small portion (7.3%) of boreal forest areas show significant positive correlation between summer NDVI and early spring (from March to April) SWE, while a relatively larger portion (13.0%) of tundra areas show significant negative correlation between summer NDVI and later spring (May) SWE (not shown).

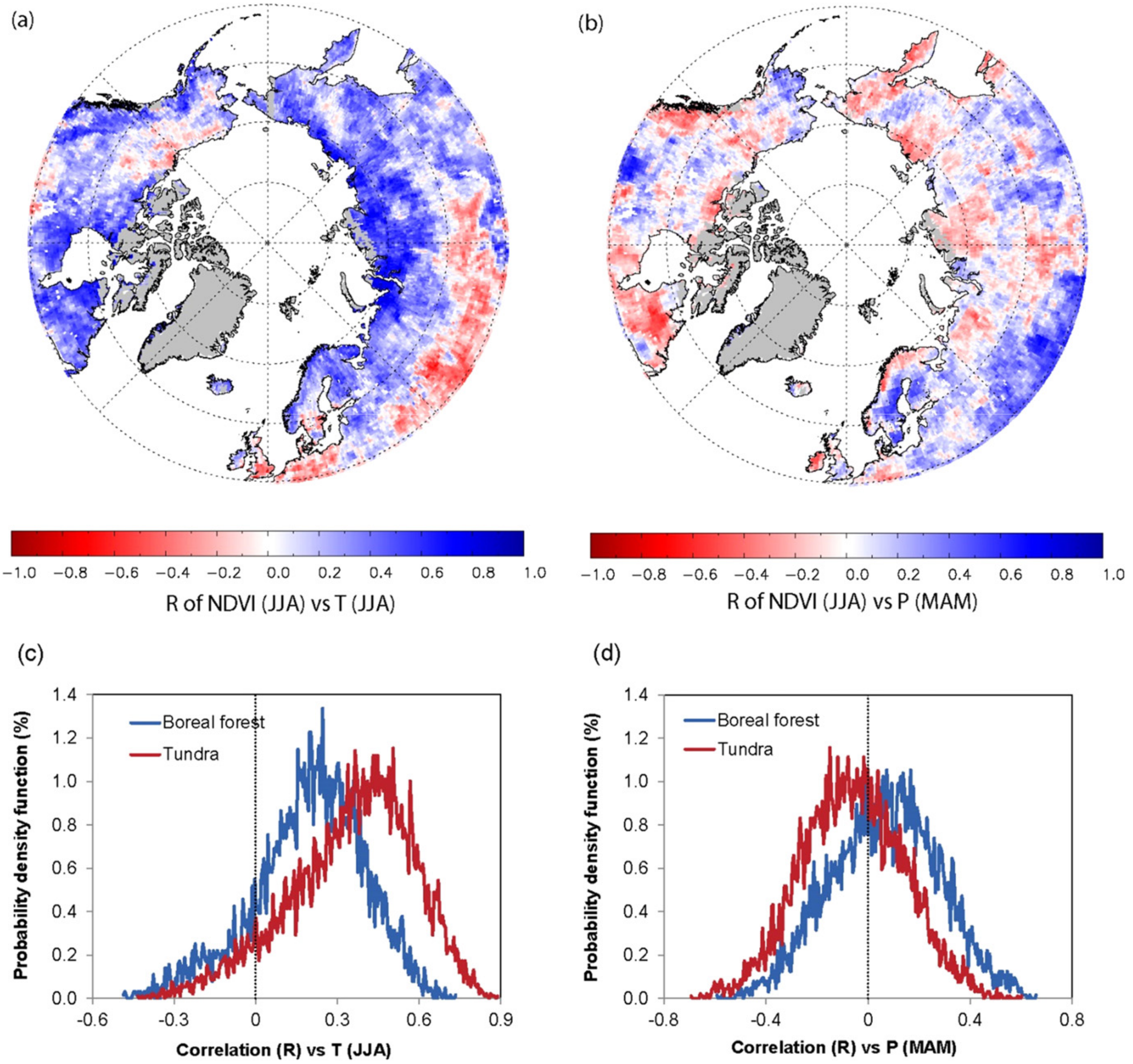

Figure 2. Sensitivity of summer NDVI changes, used as a surrogate for vegetation growth, to climate variation in the northern latitudes (⩾50° N). Maps (a) and (b) show partial correlation (*R*) patterns between summer (JJA) NDVI (GIMMS3g) anomalies versus summer air temperature (*T*, CRU) controlled by precipitation (*P*, GPCP) and spring (MAM) *P* controlled by *T* over the 1982–2010 NDVI record; areas in gray denote regions with missing data or non-vegetated areas. Plots (c) and (d) show probability density functions of the above correlation coefficients for tundra and boreal forest areas of the northern domain. For boreal forest, 29.2% and 12.5% of the pixels show significant ($p < 0.1$) positive correlation with *T* (JJA) and *P* (MAM) respectively. For tundra, 61.3% and 2.9% of the pixels show significant positive correlation with *T* (JJA) and *P* (MAM). All time series were detrended prior to the temporal correlation analysis.

These results indicate that regional warming still promotes vegetation growth, especially in tundra areas. However, the relative benefits of summer warming are lower for boreal forest than tundra ecosystems, while summer NDVI is even negatively correlated with summer air temperature (figure 2(a)) in some areas subjected to frequent disturbance, e.g. western North America (Kurz *et al* 2008). Stronger positive correlations between summer NDVI and spring *P* and SWE in boreal forest are consistent with previous studies reporting greater summer water stress in boreal forest than tundra ecosystems (Zhang *et al* 2008, Beck and Goetz 2011, Buermann *et al* 2013, Xu *et al* 2013). A negative correlation between summer NDVI and May SWE in tundra areas is likely due to a delayed onset of spring vegetation growth for years with a larger spring snow pack.

A larger impact of spring *P* and SWE on summer net carbon uptake than on summer NDVI indicates that low spring *P* or snow pack together with high summer *T* promotes fire emissions and ecosystem respiration, which may offset the relative benefits of warming on photosynthesis, and

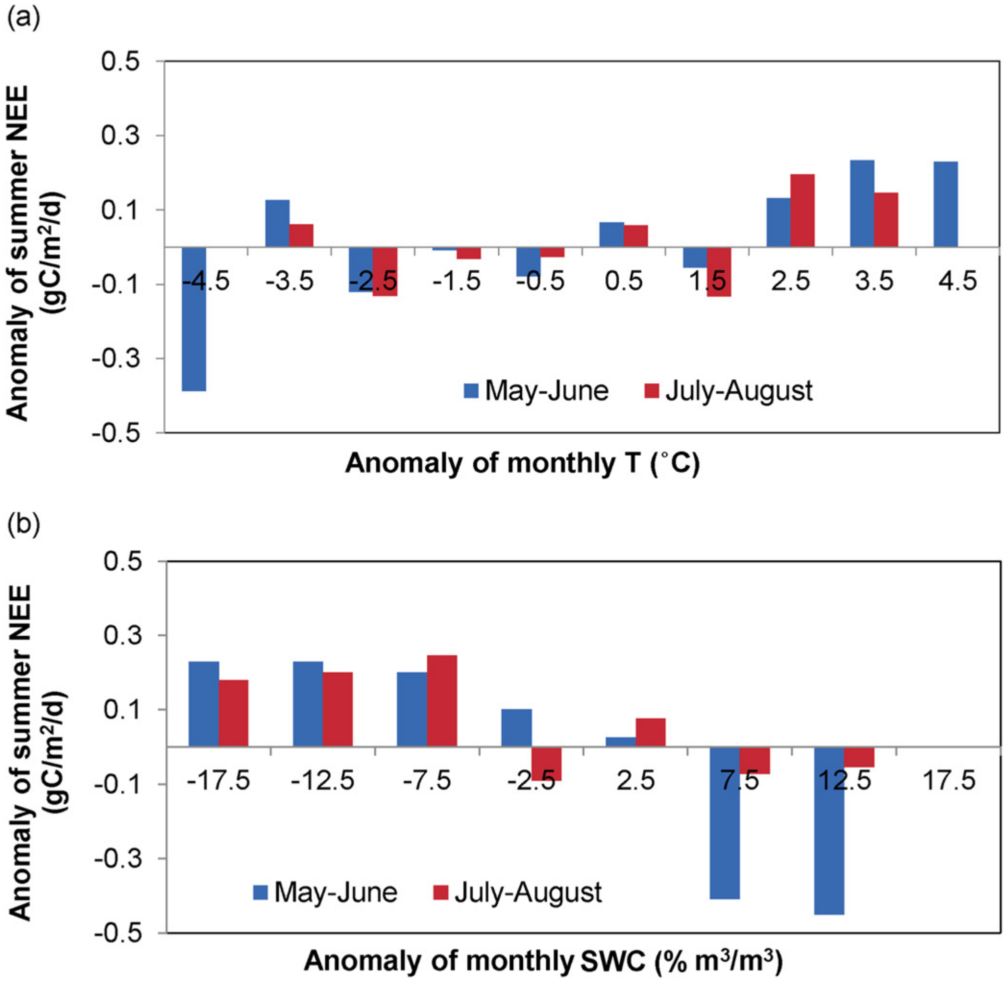

Figure 3. Tower eddy covariance data analysis for boreal North America and Northern Eurasia sites; temporal anomalies of tower measured summer (JJA) NEE fluxes are shown against (a) monthly air temperature anomalies binned into 1.0 °C intervals, and (b) surface ($\leqslant$15 cm) soil water content (SWC) anomalies binned into 0.05 m^3 m^{-3} intervals. For the air temperature analysis, there are 48, 48, 48, and 49 site-years used to represent each month from May to August, respectively; for soil moisture, there are 29, 26, 23, and 28 site-years used to represent each month from May to August. The analysis period is divided into early growing-season (May–June) and later growing-season (July–August) periods. Positive (negative) NEE anomalies denote relative reductions (increases) in terrestrial carbon uptake.

dominate the signal shown in the atmospheric CO_2 seasonal cycle. The NOAA ESRL CarbonTracker carbon flux inversion (Peters *et al* 2007) from 2000 to 2010 indicates a much smaller contribution of summer fire emissions (and also other carbon fluxes including fossil fuel emissions and air-sea gas exchange) to the interannual variability of summer atmosphere CO_2 minimums relative to terrestrial NEE contributions (figure S3), consistent with Wunch *et al* (2013). Therefore, the strong influence of spring *P* or snow (SWE) on summer net carbon uptake should mainly reflect the impact of spring hydrology on ecosystem respiration in relatively wet boreal and arctic regions, while a similar response of photosynthesis and respiration to temperature may reduce the apparent sensitivity of the residual NEE carbon flux to temperature variability (Yi *et al* 2013).

3.3. Summer NEE and spring hydrology

Figure 3 shows the anomalies of observed summer (JJA) NEE versus anomalies of monthly average *T* (figure 3(a)) and surface ($\leqslant$15 cm) soil water content (SWC) (figure 3(b)) during the growing season (from May to August) from 23 boreal ($\geqslant$50°N) EC tower sites in North America and northern Eurasia (table S1). These results indicate that boreal ecosystems tend to lose carbon under relatively warm or dry conditions. Summer NEE is generally positively correlated with growing-season *T*, and negatively correlated with growing-season SWC especially during the early growing season (from May to June, table S5). However, the correlation between summer NEE and SWC may be caused by co-variation of SWC and *T*. To examine this, we also looked at the correlation of monthly SWC and *T* anomalies. SWC only shows a marginal correlation with *T* during the growing season (table S5) except for April, where a strong positive correlation between *T* and SWC is found ($R = 0.72$, $p < 0.001$). A positive correlation between SWC and *T* in April and May is coincident with spring snowmelt and soil thawing, while SWC becomes more negatively correlated with *T* during the later growing season (July and August), likely due to greater evaporation and associated soil water loss later in the season. Therefore, the consistent negative correlation between summer NEE and growing-season SWC is unlikely to be an artifact of co-variation between T and SWC during this period. However, local conditions may also play a role in shaping the response of boreal ecosystems to climate variations. For example, summer NEE was found to increase with temperature warming at a few boreal sites in northern Europe (figure S4 and table S6), where soil and forest conditions may be quite different from boreal North America and Russia (Valentini *et al* 2000).

Further analysis using the satellite-derived (AMSR-E) surface ($\leqslant 2$ cm) soil moisture record indicates that soil moisture is closely associated with spring hydrology during the early growing season (June, figure 4), but more strongly impacted by T during the later growing season (July and August, not shown). A larger spring snow pack is generally associated with higher surface soil moisture during the early growing season (figures S5 & S6), with some exceptions (e.g. year 2010) where the surface soil moisture is more closely associated with spring precipitation. The AMSR-E soil moisture record for May is not shown due to extensive data retrieval gaps from persistent ice/snow cover and frozen soil conditions in most tundra areas, but is generally similar to the June soil moisture pattern. During the later growing season, the AMSR-E soil moisture record becomes more negatively correlated with T (July and August, mean $R = -0.14$; with 14.6% pixels showing significant correlation) than during the early season (May and June, mean $R = -0.08$; with 13.4% pixels showing significant correlation). These regional results are generally consistent with the local tower data analysis. However, it should be noted that the satellite-derived soil moisture retrievals are associated with large uncertainties and should be interpreted with caution, especially during the peak growing season under higher aboveground vegetation biomass and extensive open water inundation (Jones *et al* 2007, Yi *et al* 2011).

4. Discussion

In this study, we investigated the co-variation of seasonal climate and summer carbon uptake activity of boreal/arctic ecosystems at an annual scale. The seasonal climate variables examined included spring and summer T, P and SWE. Among all the seasonal climate variables examined, spring hydrology (P, SWE) and summer T are the two major factors that explain interannual variability in GFED fire emissions, summer net carbon uptake indicated by the atmospheric CO_2 observations, and NEE derived from model inversion (tables S2 & S4). By contrast, spring air temperature and summer precipitation have a much weaker apparent impact on annual fire emissions and summer net carbon uptake.

Our results demonstrate the important role of spring hydrology in regulating summer carbon uptake in northern ecosystems, which has been generally overlooked in previous boreal/arctic carbon cycle studies. Air temperature is considered a dominant climatic factor controlling vegetation activity and carbon uptake in boreal and arctic ecosystems (e.g. Angert *et al* 2005, Piao *et al* 2008, Zhang *et al* 2008, Yi *et al* 2010, Kim *et al* 2012, Buermann *et al* 2013). Therefore, previous studies have largely focused on how earlier spring onset and longer growing seasons associated with spring warming, and water stress induced by summer warming influence terrestrial carbon uptake. Spring warming generally promotes vegetation growth and increased net carbon uptake during the early growing season (Angert *et al* 2005, Welp *et al* 2007, Kim *et al* 2012), which is consistent with our analysis of mid-spring (May) satellite NDVI records and the timing of atmospheric CO_2 spring drawndown (not shown). Earlier spring onset associated with longer potential growing seasons and warmer temperatures may also increase atmosphere evaporative demand and vegetation drought stress during the summer, offsetting potential benefits of warmer temperatures for vegetation growth, especially in more drought-prone boreal forests (Zhang *et al* 2008, Buermann *et al* 2013, Xu *et al* 2013). Our analysis also showed a relatively weak positive correlation between mid-summer (July and August) air temperatures and boreal NDVI growth anomalies consistent with the expected greater drought sensitivity in these areas. Warmer summer temperatures and drought may also promote soil respiration and fire emissions in the boreal/arctic region (Bond-Lamberty *et al* 2007, Welp *et al* 2007, Beck and Goetz 2011). However, relatively few regional studies have examined the impact of climate variability on different components of the boreal/arctic carbon cycle beyond vegetation productivity and thus its integrated impact on net ecosystem carbon uptake.

The important role of spring hydrology in regulating summer net carbon uptake of boreal/arctic ecosystems has been documented from limited field measurements that show strong linkages between surface hydrology and water table depth variations, and net ecosystem carbon uptake (Desai *et al* 2010, Olivas *et al* 2010, Lupascu *et al* 2013, Sharp *et al* 2013). A regional analysis driven by satellite data also found that photosynthesis and respiration respond similarly to warming in the northern latitudes, thus reducing NEE sensitivity to temperature (Yi *et al* 2013). On the other hand, various components of the terrestrial carbon budget may respond differently to changes in soil water conditions. Boreal and arctic soils are generally wet and poorly drained, with relatively cold temperatures limiting soil decomposition and respiration processes (Davidson *et al* 1998, Goulden *et al* 1998). Previous field studies indicate that photosynthesis is more sensitive than ecosystem respiration to soil moisture variability or soil drought conditions (e.g. Welp *et al* 2007, Sharp *et al* 2013); however, these studies may be influenced by general assumptions about the dependence of photosynthesis and respiration on temperature and soil moisture used to partition NEE fluxes and for temporal gap filling, and general difficulties obtaining extensive measurements of carbon fluxes in the northern latitudes. More detailed analyses and understanding of carbon flux sensitivity to soil hydrology are constrained by sparse observations of these processes in boreal/arctic ecosystems.

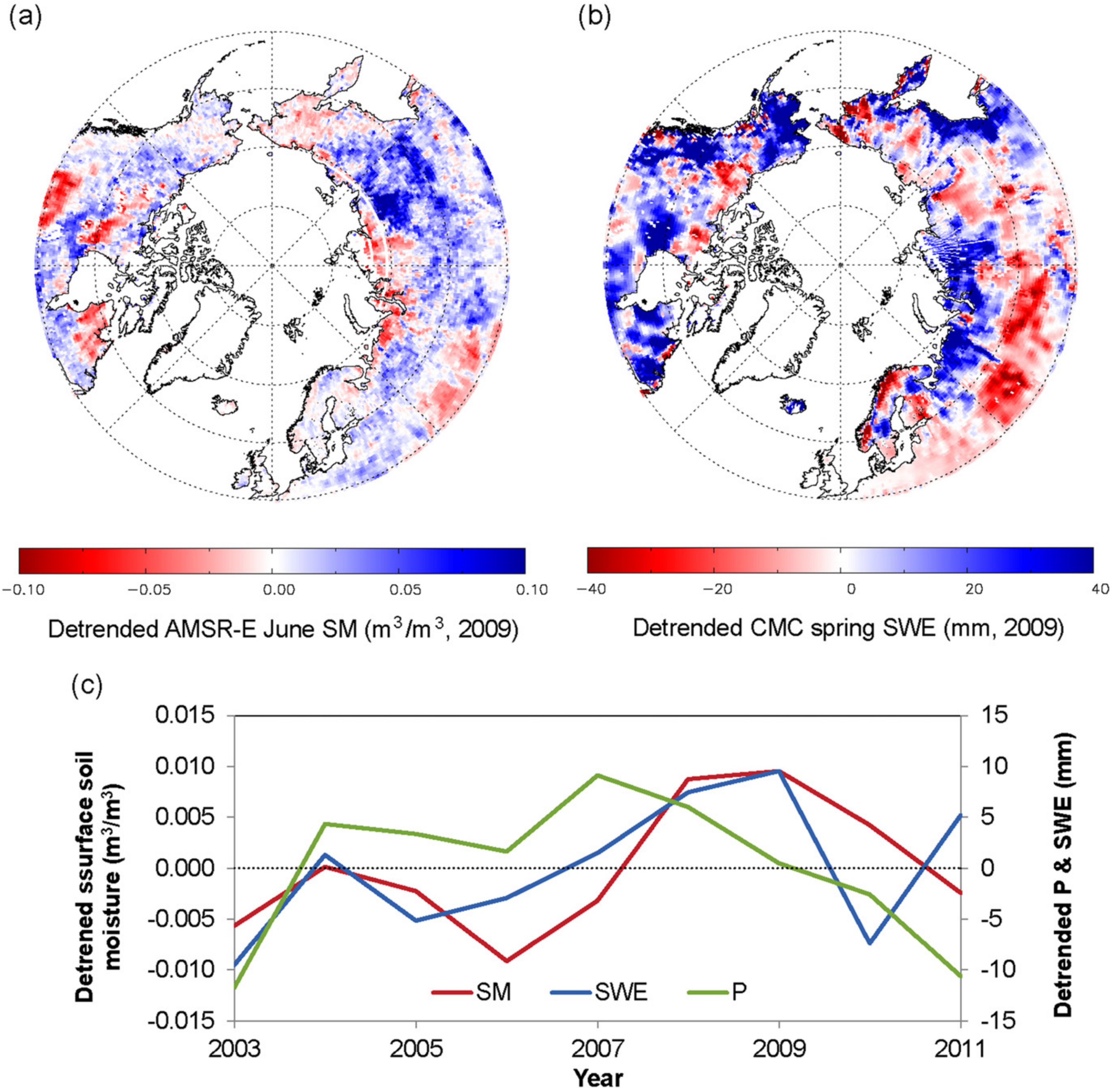

Figure 4. Co-variation of AMSR-E retrieved surface ($\leqslant$2 cm) soil moisture (SM) in June and spring (MAM) hydrology (P & SWE). The spatial patterns of detrended SM (a) and SWE (b) for a particularly wet year (2009) are shown. The detrended time series (2003–2011) of regional mean SM, SWE and P are shown in (c). Large spring precipitation or snow pack anomalies generally correspond with high surface soil moisture in June.

Approximately 12.8% to 17.8% of the exposed land area in the Northern Hemisphere is underlain by permafrost (mostly distributed in the boreal/arctic domain; Zhang *et al* 2000). These areas contain extensive soil organic carbon stocks that may be vulnerable to increased mobilization and decomposition from near term climate warming (Schuur *et al* 2009, Tarnocai *et al* 2009). The potential sensitivity and rate of carbon emissions from these changes are uncertain, but are closely tied with surface hydrology and associated moisture and temperature controls to soil decomposition and permafrost degradation (Lupascu *et al* 2013). Spring snow cover and surface soil moisture are among the main factors influencing permafrost temperature and active layer depth (Zhang *et al* 2005). Permafrost degradation can also alter surface moisture conditions independent of regional precipitation (Smith *et al* 2005, Velicogna *et al* 2012). These factors may partially explain the relatively strong correspondence of spring hydrology (and the weaker correspondence of summer P) with the regional carbon cycle reported in this study.

Our analysis of the atmospheric CO_2 observations assumes that northern terrestrial ecosystems have a dominant influence on the CO_2 seasonal cycle above 50°N, while other studies have demonstrated that mid-latitude temperate ecosystems can also have a sizable influence on these processes (e.g. Randerson *et al* 1997, Graven *et al* 2013, Wunch *et al* 2013). The study of Wunch *et al* (2013) indicated covariance of column-averaged summer CO_2 minimums from Northern Hemisphere TCCON (Total Carbon Column Observing Network) and GOSAT (Greenhouse gases Observing SATellite) observations, with August temperatures averaged from 30°N to 60°N. The relatively strong correspondence between summer T and atmosphere CO_2 indicated by Wunch *et al* (2013) is likely due to large-scale, temperature-related dynamical mixing in the atmosphere and relatively strong sensitivity of ecosystem summer net carbon uptake to temperature and drought in the mid-latitudes, especially later in the growing season (Angert *et al* 2005, Piao *et al* 2008, Yi *et al* 2010). Underestimated seasonality of fossil fuel emissions (Gurney *et al* 2005) and increasing northern energy development during the last decade may also influence the atmospheric CO_2 seasonal cycle, though our analysis of CarbonTracker simulations from 2000 to 2010 showed a relatively small impact of fossil fuel emissions relative to terrestrial ecosystems during that period (figure S3). On the other hand, the Bayesian atmospheric inversion model analysis indicates a large impact of summer temperature on the net carbon uptake of northern ecosystems compared to a negligible summer temperature influence on the northern atmospheric CO_2 summer minimum. However, atmospheric inversion models generally have difficulties in locating a carbon sink within a continent due to sparse atmospheric CO_2 observations and large uncertainties in atmospheric transport modeling (Gurney *et al* 2008).

The regional climate data used in this study are associated with large uncertainties due to sparse weather station networks, difficulties in measuring snowfall with gauges, and the generally lower accuracy of satellite-based precipitation, snow and soil moisture retrievals in the northern high latitudes (e.g. Adler *et al* 2012, Dong *et al* 2005, Yi *et al* 2011). A set of new NASA hydrology missions, including SMAP (Soil Moisture Active and Passive, Entekhabi *et al* 2010) and GPM (Global Precipitation Measurement, Smith *et al* 2007), are expected to provide global measurements of surface ($\leqslant$5 cm) soil moisture and precipitation, respectively, with improved accuracy and spatial resolution (less than ~10 km); the Orbiting Carbon Observatory (OCO-2) is designed to collect global measurements of vertical atmospheric CO_2 profiles at much higher resolution and precision than current sparse atmospheric observation networks (Boesch *et al* 2011). These new observational capabilities are expected to enable improved regional hydrological and ecological analyses, and understanding of regional CO_2 sources and sinks, and their associated climate sensitivity.

5. Conclusions

Our work illuminates the important role of spring hydrology in determining summer net carbon uptake even in predominantly temperature-limited high-latitude ecosystems. Large precipitation or snow cover conditions in spring generally promote summer net carbon uptake independent of air temperature effects as indicated by both the atmospheric CO_2 seasonal cycle and tower EC measurements. In contrast, satellite NDVI measurements still indicate an overall benefit of summer vegetation growth from warming. This discrepancy is attributed to the similar response of photosynthesis and respiration to temperature, resulting in reduced temperature sensitivity of the residual net carbon flux. On the other hand, spring precipitation and snow cover are closely related to surface soil moisture during the early growing season, exerting a strong control on soil respiration in relatively wet boreal and arctic ecosystems. Spring precipitation also strongly regulates summer fire emissions in the high latitudes, which may become more important to the regional carbon budget with continued warming. Spring hydrology is therefore likely to have an increasing impact on the northern carbon cycle under current climate trends and projections of increasing cold season precipitation and magnified warming trends over the northern high latitudes. If current warming trends continue, the regional carbon and water cycles may become more closely coupled as northern ecosystems switch from primarily energy limited to stronger water limitations for vegetation growth and carbon sink activity.

Acknowledgments

This study used tower eddy covariance data acquired by the FLUXNET community, which was supported by the CarboEuropeIP, FAO-GTOS-TCO, iLEAPS, Max Planck Institute for Biogeochemistry, National Science Foundation, University of Tuscia, Université Laval and Environment Canada, US Department of Energy and NOAA ESRL, as well as many local funders. The authors thank Dr F Chevallier for providing the Bayesian model inversion results. Funding for this study was provided by the NASA Earth Science program (NNX11AD46G).

References

Adler R F, Gu G and Huffman G J 2012 Estimating climatological bias errors for the Global Precipitation Climatology Project (GPCP) *J. Appl. Meteor. Climatol.* **51** 84–99

Angert A, Biraud S, Bonfils C, Henning C C, Buermann W, Pinzon J, Tucker C J and Fung I 2005 Drier summers cancel out the CO_2 uptake enhancement induced by warmer springs *Proc. Natl. Acad. Sci. USA* **102** 10823–7

Baldocchi D 2008 Breathing of the terrestrial biosphere: lessons learned from a global network of carbon dioxide flux measurement systems *Aust. J. Bot.* **56** 1–26

Beck P S and Goetz S J 2011 Satellite observations of high northern latitude vegetation productivity changes between 1982 and 2008: ecological variability and regional differences *Environ. Res. Lett.* **6** 045501

Boesch H, Baker D, Connor B, Crisp D and Miller C 2011 Global characterization of CO_2 column retrievals from shortwaveinfrared satellite observations of the orbiting carbon observatory-2 mission *Remote Sens.* **3** 270–304

Bond-Lamberty B, Peckham S D, Ahl D E and Gower S T 2007 Fire as the dominant driver of central Canadian boreal forest carbon balance *Nature* **450** 89–92

Brown R D and Brasnett B 2010 Canadian Meteorological Centre (CMC) Daily Snow Depth Analysis Data (Boulder, CO: National Snow and Ice Data Center)

Buermann W, Bikash P R, Jung M, Burn D H and Reichstein M 2013 Earlier springs decrease peak summer productivity in North American boreal forests *Environ. Res. Lett.* **8** 024027

Chevallier F *et al* 2010 CO_2 surface fluxes at grid point scale estimated from a global 21 year reanalysis of atmospheric measurements *J. Geophys. Res.* **115** D21307

Davidson E A, Belk E and Boone R D 1998 Soil water content and temperature as independent or confounded factors controlling soil respiration in a temperate mixed hardwood forest *Glob. Change Biol.* **4** 217–27

Desai A R, Helliker B R, Moorcroft P R, Andrews A E and Berry J A 2010 Climatic controls of interannual variability in regional carbon fluxes from top-down and bottom-up perspectives *J. Geophys. Res.* **115** G02011

Dong J, Walker J P and Houser P R 2005 Factors affecting remotely sensed snow water equivalent uncertainty *Remote Sens. Environ.* **97** 68–82

Entekhabi D *et al* 2010 The Soil Moisture Active Passive (SMAP) mission *Proc. IEEE* **98** 704–16

Flanagan L B and Syed K H 2011 Stimulation of both photosynthesis and respiration in response to warmer and drier conditions in a boreal peatland ecosystem *Glob. Change Biol.* **17** 2271–87

Friedl M A, Sulla-Menashe D, Tan B, Schneider A, Ramankutty N, Sibley A and Huang X 2010 MODIS Collection 5 global land cover: Algorithm refinements and characterization of new datasets *Remote Sens. Environ.* **114** 168–82

Goulden M *et al* 1998 Sensitivity of boreal forest carbon balance to soil thaw *Science* **279** 214–7

Graven H *et al* 2013 Enhanced seasonal exchange of CO_2 by northern ecosystems since 1960 *Science* **341** 1085–9

Gurney K R, Baker D, Rayner P and Denning A S 2008 Interannual variations in regional net carbon exchange and sensitivity to observing networks estimated from atmospheric CO_2 inversions for the period 1979 to 2006 *Glob. Biogeochem. Cycles* **22** GB3025

Gurney K R, Chen Y H, Maki T, Kawa S R, Andrews A and Zhu Z 2005 Sensitivity of atmospheric CO_2 inversions to seasonal and interannual variations in fossil fuel emissions *J. Geophys. Res.* **110** D10308

Harris I, Jones P D, Osborn T J and Lister D H 2013 Updated high-resolution grids of monthly climatic observations—the CRU TS3.10 Dataset *Int. J. Climatol.* **34** 623–42

Jones L A and Kimball J S 2010 Daily Global Land Surface Parameters (Boulder, CO: National Snow and Ice Data Center)

Jones L A, Kimball J S, McDonald K C, Chan S K, Njoku E G and Oechel W C 2007 Satellite microwave remote sensing of boreal and Arctic soil temperatures from AMSR-E *IEEE Trans. Geosci. Remote Sens.* **45** 2004–18

Kim Y, Kimball J S, Zhang K and McDonald K C 2012 Satellite detection of increasing Northern Hemisphere non-frozen seasons from 1979 to 2008: implications for regional vegetation growth *Remote Sens. Environ.* **121** 472–87

Kurz W A, Dymond C C, Stinson G, Rampley G J, Neilson E T, Carroll A L, Ebata T and Safranyik L 2008 Mountain pine beetle and forest carbon feedback to climate change *Nature* **452** 987–90

Lupascu M, Welker J M, Seibt U, Maseyk K, Xu X and Czimczik C I 2013 High arctic wetting reduces permafrost carbon feedbacks to climate warming *Nat. Clim. Change* **4** 51–5

Masarie K A and Tans P P 1995 Extension and integration of atmospheric carbon dioxide data into a globally consistent measurement record *J. Geophys. Res.* **100** 11593–610

McGuire A D *et al* 2012 An assessment of the carbon balance of arctic tundra: comparisons among observations, process models, and atmospheric inversions *Biogeosciences* **9** 3185–204

Olivas P C, Oberbauer S F, Tweedie C E, Oechel W C and Kuchy A 2010 Responses of CO_2 flux components of alaskan coastal plain tundra to shifts in water table *J. Geophys. Res.* **115** G00I05

Peters W *et al* 2007 An atmospheric perspective on North American carbon dioxide exchange: carbon tracker *Proc. Natl. Acad. Sci. USA* **104** 18925–30

Piao S *et al* 2008 Net carbon dioxide losses of northern ecosystems in response to autumn warming *Nature* **451** 49–52

Randerson J T, Thompson M V, Conway T J, Fung I Y and Field C B 1997 The contribution of terrestrial sources and sinks to trends in the seasonal cycle of atmospheric carbon dioxide *Glob. Biogeochem. Cycles* **11** 535–60

Schuur E A G, Vogel J G, Crummer K G, Lee H, Sickman J O and Osterkamp T E 2009 The effects of permafrost thaw on old carbon release and net carbon exchange from tundra *Nature* **459** 556–9

Sharp E D, Sullivan P F, Steltzer H, Csank A Z and Welker J M 2013 Complex carbon cycle responses to multi-level warming and supplemental summer rain in the high arctic *Glob. Change Biol.* **19** 1780–92

Smith E A *et al* 2007 International Global Precipitation Measurement (GPM) program and mission: an overview *Measuring Precipitation from Space: Eurainsat and the Future* ed V Levizzani, P Bauer and F J Turk (Berlin: Springer) pp 611–54

Smith L C, Sheng Y, MacDonald G M and Hinzman L D 2005 Disappearing arctic lakes *Science* **308** 1429

Solomon S, Qin D, Manning M, Marquis M, Averyt K, Tignor M M B, Miller Jr H L and Chen Z 2007 *Climate Change 2007: The Physical Science Basis* (Cambridge: Cambridge University Press) p 996

Tarnocai C, Canadell J G, Schuur E A G, Kuhry P, Mazhitova G and Zimov S 2009 Soil organic carbon pools in the northern circumpolar permafrost region *Global Biogeochem. Cycles* **23** GB2023

Thoning K W, Tans P P and Komhyr W D 1989 Atmospheric carbon dioxide at mauna loa observatory, 2. Analysis of the NOAA/GMCC data, 1974–1985 *J. Geophys. Res.* **94** 8549–65

Valentini R *et al* 2000 Respiration as the main determinant of carbon balance in European forests *Nature* **404** 861–5

van der Werf G R, Randerson J T, Giglio L, Collatz G J, Mu M, Kasibhatla P S, Morton D C, DeFries R S, Jin Y and van Leeuwen T T 2010 Global fire emissions and the contribution of deforestation, savanna, forest, agricultural, and peat fires (1997–2009) *Atmos. Chem. Phys.* **10** 11707–35

Velicogna I, Tong J, Zhang T and Kimball J S 2012 Increasing subsurface water storage in discontinuous permafrost areas of the Lena River basin, Eurasia, detected from GRACE *Geophys. Res. Lett.* **39** L09403

Welp L R, Randerson J T and Liu H P 2007 The sensitivity of carbon fluxes to spring warming and summer drought depends on plant functional type in boreal forest ecosystems *Agric. For. Meteorol.* **147** 172–85

Wunch D *et al* 2013 The covariation of Northern Hemisphere summertime CO_2 with surface temperature in boreal regions *Atmos. Chem. Phys.* **13** 9447–59

Xu L *et al* 2013 Temperature and vegetation seasonality diminishment over northern lands *Nat. Clim. Change* **3** 581–6

Yi C *et al* 2010 Climate control of terrestrial carbon exchange across biomes and continents *Environ Res. Lett.* **5** 034007

Yi Y, Kimball J S, Jones L A, Reichle R H and McDonald K C 2011 Evaluation of MERRA land surface estimates in preparation for the soil moisture active passive mission *J. Climate* **24** 3797–816

Yi Y, Kimball J S, Jones L A, Reichle R H, Nemani R and Margolis H A 2013 Recent climate and fire disturbance impacts on boreal and arctic ecosystem productivity estimated using a satellite-based terrestrial carbon flux model *J. Geophys. Res.* **118** 606–22

Yue S, Pilon P, Phinney B and Cavadias G 2002 The influence of autocorrelation on the ability to detect trend in hydrological series *Hydrol. Process.* **16** 1807–29

Zhang K, Kimball J S, Hogg E H, Zhao M, Oechel W C, Cassano J J and Running S W 2008 Satellite-based model detection of recent climate-driven changes in northern high-latitude vegetation productivity *J. Geophys. Res.* **113** G03033

Zhang T *et al* 2005 Spatial and temporal variability in active layer thickness over the Russian arctic drainage basin *J. Geophys. Res.* **110** D16101

Zhang T, Heginbottom J A, Barry R G and Brown J 2000 Further statistics on the distribution of permafrost and ground ice in the northern hemisphere *Polar Geogr.* **24** 126–31